Published in final edited form as:
J Alloys Compd. 2020 September 5; 834: . doi:10.1016/j.jallcom.2020.154987.

Welding and Additive Manufacturing with Nanoparticle-Enhanced Aluminum 7075 Wire

Daniel Oropeza[a,1], **Douglas C. Hofmann**[a], **Kyle Williams**[a], **Samad Firdosy**[a], **Punnathat Bordeenithikasem**[a,*], **Maximillian Sokoluk**[b], **Maximilian Liese**[b], **Jingke Liu**[b], **Xiaochun Li**[b,c]

[a)]Engineering and Science Directorate, Jet Propulsion Laboratory, California Institute of Technology, 4800 Oak Grove Dr, Pasadena, CA 91109, USA

[b)]Department of Mechanical and Aerospace Engineering, University of California, Los Angeles, 420 Westwood Plaza, Los Angeles, CA 90095, USA

[c)]Department of Materials Science and Engineering, University of California, Los Angeles, 410 Westwood Plaza, Los Angeles, CA 90095, USA

Abstract

Aluminum alloy 7075 (Al 7075) with a T73 heat treatment is commonly used in aerospace applications due to exceptional specific strength properties. Challenges with manufacturing the material from the melt has previously limited the processing of Al 7075 via welding, casting, and additive manufacturing. Recent research has shown the capabilities of nanoparticle additives to control the solidification behavior of high-strength aluminum alloys, showcasing the first Al 7075 components processed via casting, welding, and AM. In this work, the properties of nanoparticle-enhanced aluminum 7075 are investigated on welded parts, overlays and through wire-based additive manufacturing. The hardness and tensile strength of the deposited materials were measured in the as-welded and T73 heat-treated conditions showing that the properties of Al 7075 T73 can be recovered in welded and layer-deposited parts. The work shows that Al 7075 now has the potential to be conventionally welded or additively manufactured from wire into high-strength, crack-free parts.

Graphical abstract

[*]**Corresponding Author:** P.B.: punnathat.bordeenithikasem@jpl.nasa.gov.
[1]Present address: Department of Mechanical Engineering, Massachusetts Institute of Technology, 32 Vassar St, Room 35-214, Cambridge, MA 02139 USA

Author Contributions

X.L. and M.S. designed the welding wire material. X.L. supervised the fabrication of the wire in MetaLi LLC. M.L. and J.L. optimized the post treatment of the wire. K.W. fabricated the weld, overlay, and 3D printed samples. D.O. performed the hardness and microstructure characterization experiments. D.O., D.C.H., and P.B. performed the tensile experiments. S.F. assisted with sample etching for microstructural analysis. D.O. performed the data analysis for the hardness, microstructure, and tensile experiments. The results were discussed by D.O., D.C.H., S.F., X.L. and P.B. The manuscript was written by D.O., D.C.H., and P.B. The figures were produced by D.O.

Competing Interests

The author(s) declare no competing interests.

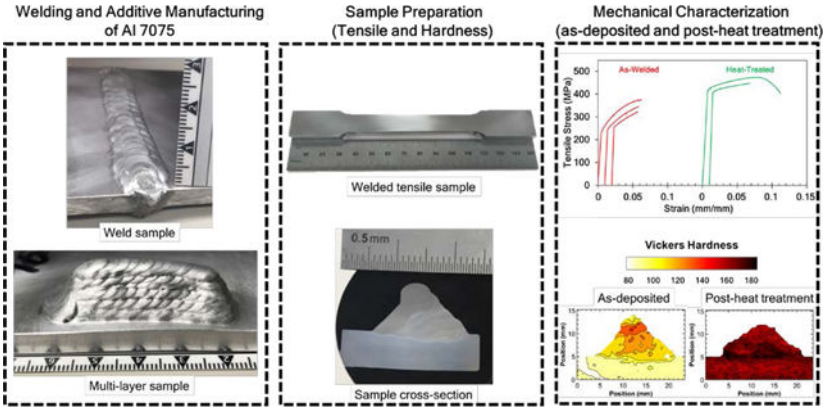

Keywords

Aluminum 7075; arc welding; wire-fed additive manufacturing; 3D printing

1. Introduction

Aluminum alloys are ubiquitous engineering materials, having applications in automobiles, aircraft, spacecraft, heat exchangers, and components for machines and manufacturing equipment due to high specific strength, favorable oxidation and corrosion properties, and high electrical and thermal conductivity [1–5]. Of particular use in high-strength applications is the aluminum alloy 7075 (Al 7075), containing alloying elements of zinc, magnesium, and copper, resulting in exceptional specific strength properties [1,6,7]. This alloy is used extensively in aerospace applications, ranging from aircraft wing spars to spacecraft chassis to planetary rover wheels [2–5]. Despite its impressive mechanical properties, aluminum 7075 is a precipitation-hardened alloy that requires precise control over its strengthening phases and is also prone to solidification cracking. This has limited the manufacturing potential of the alloy for aerospace components from the melt, such as in casting, welding and additive manufacturing. For example, Al 7075 is difficult to join via traditional welding methods (e.g., tungsten inert gas or TIG, metal inert gas or MIG) due to solidification cracking and over-aging of precipitates [1,7–10]. As a result, aerospace components of Al 7075 are typically machined from billets and assemblies are bolted or brazed instead of conventionally arc welded, which is not currently flight qualified for spacecraft components.

Recently, advances in nanoparticle additives for aluminum alloys have resulted in control of grain nucleation and growth during solidification [11–14]. This is achieved by selecting nanoparticles with similar crystal structure and minimal lattice mismatch for the primary solidification phase of the alloy, resulting in a reduced nucleation energy barrier during solidification and leading to heterogeneous nucleation and a final microstructure composed of small equiaxed grains [11,15]. By producing small equiaxed grains during solidification, as opposed to columnar dendritic grains which can trap liquid between solidified grains, the thermal strain of solidification can be mitigated and thus prevention of void formation and hot tearing is possible [11,15–17]. Additionally, it is believed that the addition of

nanoparticles can help prevent grain growth during heat treatment through grain boundary pinning, thus producing small equiaxed grains after solidification from the melt and heat treatments [11]. In 2013, Choi *et al* first used nanoparticles to eliminate hot tearing in the hot tear susceptible aluminum cast alloy A206 (Al-4.5Cu-0.25Mg) [16]. In 2017, a group from HRL and colleagues reported the ability to produce crack-free aluminum 6061 and 7075 parts processed via the additive manufacturing (AM) process of laser powder bed fusion (LPBF) through the use of ZrH_2 nanoparticle additives [15]. In 2019, a group led by UCLA reported on the possibility of controlling the microstructure of Al 7075 for casting and studied the effect of a T6 heat treatment on the microstructure through the use of TiC nanoparticles [11]. Also in 2019, the same group from UCLA published the development of a TiC nanoparticle-enhanced Al 7075 weld wire, showcasing the possibility to form crack-free welds of Al 7075 using this weld wire and the return of mechanical properties (i.e., hardness and tensile strength) of the weld component after T6 heat treatment [17]. A more detailed summary of the influence of nanoparticles on the solidification behavior of nano-particle enhanced Al 7075 weld wire can be found in the work of Zuo *et. al* [11] and Sokoluk *et. al* [17].

To increase the broad applicability of Al 7075 in future aerospace hardware, a full suite of manufacturing capabilities are required, including machining, welding, casting, and additive manufacturing (from multiple feedstock sources such as powder, wire, molten metal, and sheetmetal). AM has gained attention from various industries due to the possibility of fabricating complex three-dimensional geometries that would be otherwise difficult or impossible to fabricate via conventional manufacturing practices [18]. Metal AM in particular has garnered interest from automobile, healthcare, and aerospace industries for the production of complex components, in small production runs, with short lead time [19,20]. The development of aluminum alloys for AM has been much slower than other metal alloys such as titanium, steel and Inconel due largely to the difficulty with melting and solidifying crack-free aluminum alloys using laser-based systems and the relative ease by which aluminum can be machined. The vast majority of all aluminum used in metal AM is the adapted casting alloy AlSi10Mg [21], which is normally fabricated from powder using LPBF [19]. Despite recent advances in the printing of high-strength Al 7075 and Al 6061 through powder bed fusion, wire-based additive manufacturing of these alloys has not yet been widely successful. Compared to powder-based processes, wire-based metal AM has benefits in material handling safety, increased material deposition rate, and larger build envelopes [21–24]. A detailed summary of wire-based additive manufacturing is provided by Rodrigues *et. al* [23]. As both welding and fusion-based AM processes require the joining of metallic feedstock through significant energy deposition, material melting and solidification, it is not surprising that the processing of aluminum alloys via AM and welding share similar challenges of solidification cracking, residual stresses, and complex microstructure formation [25]. As a result of processing challenges, there has been a growing interest in the development of new alloys specifically for fusion based AM processes, and in particular for wire-based AM [15,26,27].

In this work, we demonstrate conventional TIG butt welding of Al 7075 T73, using standard flight welding procedures using a certified flight welder with nanoparticle-enhanced Al 7075 weld wire provided by MetaLi LLC. We measure the tensile strength, ductility, and explore

the microstructure of samples in the as-welded condition and after T73 heat treatment. Although T6 heat treatments have been demonstrated previously [17], the T73 heat treatment is more commonly utilized for spacecraft components due to improved stress corrosion cracking (SCC) properties when compared to T6 [1,4,18]. Because of potentially corrosive environments experienced by aircraft and spacecraft during storage and operation [28,29], and the serious nature of failure by SCC, resistance to stress corrosion cracking is of critical importance to aerospace components [28]. Both tempers involve solution heat treatment, but while the T6 temper artificially ages the material to form fine and continuous precipitates for peak strength, the T73 temper utilizes an over-aging treatment to form discontinuous and coarse precipitates at the grain boundary [18,30,31]. Therefore, the microstructure and mechanical properties created by these two heat treatments are different and experiments for Al 7075 T73 are necessary. Furthermore, we investigate the effect on microstructure and hardness of the weld wire and parent material using a single pass overlay of wire onto Al 7075 T7351 plate before and after T73 heat treatment. Finally, we explore the possibility of wire-arc additive manufacturing of Al 7075 by building a multi-layer part using hand welding to simulate a wire-fed additive manufacturing process – investigating cracking, hardness and microstructure before and after T73 heat treatment. The three different fabricated samples are shown in Figure 1: (1) a conventional butt weld, (2) a single pass overlay, and (3) a multi-pass 3D printed part. The work showcases the ability of a post T73 heat-treated welded or deposited sample of nanoparticle-enhanced Al 7075 to return the mechanical properties of wrought Al 7075 T73.

2. Materials and methods

A meter of 3.2 mm diameter TiC nanoparticle-enhanced aluminum 7075 weld wire (MetaLi LLC) and 6.35 mm thick plate of aluminum 7075 T7351 (Tri-Tech Metals) were utilized for this study. More information on the composition of the nanoparticle-enhanced weld wire can be found in the paper by Sokoluk *et al* [17]. Three different samples were fabricated for this study: (1) a conventional butt weld, (2) a single pass overlay, and (3) a multi-pass 3D printed part (Figure 1). All samples were fabricated via tungsten inert gas welding using standard flight welding procedures using a certified flight welder. The welding parameters for the fabrication of the samples are shown in Table 1.

To fabricate the conventional butt weld a total of 7 passes were performed to complete the infill. The overlay sample was fabricated from a single deposition pass. The 3D printed component was made via a total of 13 deposition passes, with a base of 4 passes and 6 total layers in the vertical direction. The initial feedstock wire, schematics of the different builds and images of the fabricated parts are shown in Figure 1.

The conventional butt weld sample was cut perpendicular to the weld direction. One half of the plate was left in the as-welded condition and the other half was sent for T73 heat treatment at a commercial vendor. The as-welded and heat-treated butt weld samples were then machined into dog-bone specimens for use in tensile tests and cross-sectional samples for use in hardness and microstructure analysis. The overlay sample was cross-sectioned perpendicular to the overlay direction. One cross-sectional sample was left in the as-overlayed condition and another cross-sectional sample was sent for T73 heat treatment. The

3D printed sample was cross-sectioned perpendicular to the primary weld direction. One cross-sectional sample was left in the as-printed condition and another cross-sectional sample was sent for T73 heat treatment. Vickers' hardness tests were performed using an LM 248AT Microhardness Tester (LECO Corp), with an indentation force of 500 gf, a dwell time of 10 seconds, and indent spacing of 0.025 inches (0.625 mm). Microstructures were characterized by etching in Keller's reagent to reveal grain boundaries. Tension tests were performed using an Instron 5969 Universal Testing Machine with a 50kN load cell and a crosshead displacement of 0.2 mm/min. An extensometer was used to measure the strain of the sample up to 3 mm of displacement. The dog-bone tensile samples were machined to shape and featured a gauge length of 80mm, a nominal thickness of 6 mm and a nominal width of 12 mm. Exact cross-sectional dimensions for each sample were used to calculate stress and strain values, with yield strength reported for the 0.2% strain offset method. Three tensile samples of as-received aluminum 7075 T7351 plate, three tensile samples of the conventional butt weld in the as-welded condition, and two tensile samples of the conventional butt weld in the T73 heat-treated condition were fabricated and tested.

3. Results

3.1 Hardness mapping for Al 7075 fabricated samples before and after T73 heat treatment

Vicker's hardness measurements were performed for wire and plate feedstock, as well as the weld, overlay, and 3D printed sample before and after the T73 heat treatment to develop a hardness map. Optical images of all hardness samples, along with corresponding hardness mappings before and after heat treatment are shown in Figure 2.

For the initial Al 7075 plate, a similar hardness was observed in the before and after heat treatment conditions. This is to be expected since the as-received Al 7075 plate has undergone an initial T7351 heat treatment that follows the same thermal history as the T73 treatment with additional mechanical strain relief [18]. For the TiC nanoparticle-enhanced Al 7075 weld wire, an increase in hardness from the as-received condition (124 ± 2 HV) to the heat-treated condition (167 ± 4 HV) was observed. For the butt weld, a solid interface was achieved without any measurable cracking or porosity, see Figure. 2. In the as-welded condition, the lowest hardness was in the heat affected zone (HAZ) on both sides of the weld, due to induced microstructural changes to the precipitates from the deposited thermal energy [32]. The average hardness of the weld was (117 ± 12 HV) and the average hardness of the plate near the weld was (102 ± 7HV). After the T73 heat treatment on the weld, both the plate and the HAZ returned to the nominal hardness of the unwelded plate (165 ± 5 HV). To test the effect of annealing on the initial plate, a single pass overlay was performed and the hardness was measured before and after T73 heat treating. Even after only one pass, there was a significant decrease in the hardness of the plate for at least several centimeters on both sides of the overlay. The hardness of the plate in the HAZ dropped from 168 HV to approximately 104 HV in both the overlay and in the HAZ. However, the entire plate was returned to the nominal Al 7075 T73 after heat treatment. Lastly, the 3D printed sample showed a fully dense and crack free microstructure with significant annealing in the plate, down to an average value of 95 ± 5 HV throughout the entire plate. There was some variance in hardness in the 13 layers of the build due to cooling rate changes through the layers.

However, after heat treatment, the hardness of the 3D printed region and the plate were returned to 163 ± 9 HV, which was similar to the parent material. A selected summary of the hardness properties of all samples can be seen in Table 2.

3.2 Microstructure of Al 7075 fabricated samples before and after T73 heat treatment

To understand the effects of the various sample fabrication processes on microstructure, optical micrographs of etched samples were taken for the conventional butt weld, overlay, and 3D printed samples in the before and after heat treatment conditions, shown in Figure 3.

For the butt weld before T73 heat treatment, we see an equiaxed grain structure induced by the addition of the TiC nanoparticles for the weld metal region, matching the results demonstrated by Sokoluk *et. al* [17]. Highly defined grain boundaries with larger grains in the root (bottom) of the weld than the face (top) of the weld are visible, likely the result of grain growth associated with heating of subsequent layers during additional welding passes. The grains structure is representative of a binary alloy that has formed under slow cooling conditions, with a primary solidification phase surrounded by the secondary solidification phase [33]. At the weld interface, a disruption to the parent material grain structure was observed, with enlarged columnar grains and more defined grain boundaries, likely the result of overaged coarsening of the plate grains. After the T73 heat treatment, there were less defined grain boundaries and some growth to the equiaxed grains in the weld material. The heat treatment succeeds in redistribution of the precipitates from the grain boundaries to the grains. For the single layer overlay and 3D printed sample, we see a similar microstructure before and after T73 heat treatment as for the conventional butt weld sample. Equiaxed grains form in the weld metal, with well-defined grain boundaries suggesting the alloy precipitates have solidified in the grain boundary. Comparing the 3D printed and single layer overlay microstructures in the as-printed condition, for regions of the weld metal near the base of the print (i.e., material that experienced multiple depositions of energy during the build process) we see larger grains with a textured structure for the 3D printed sample. This is due to grain growth of the originally equiaxed grains during energy deposition from subsequent layers, as well as the preferential direction of heat transfer towards the baseplate during solidification. After T73 heat treatment, the grain boundary becomes less pronounced, suggesting the precipitates have been relocated into the grains as a result of the quenching and annealing processes.

3.3 Mechanical properties of Al 7075 welded samples before and after T73 heat treatment

To determine the yield strength and ductility of the welds and to estimate the strength of the 3D printed material, tensile tests were performed on the parent as-received Al 7075 T7351 plate, as-welded, and post-weld T73 heat-treated samples. The stress-strain curves and fracture surfaces for selected experimental samples are shown in Figure 4.

The tension tests of the as-received Al 7075 T7351 plate material exhibit nominal properties reported for this alloy, including a 414 MPa yield strength, 468 MPa ultimate strength, and 11% total strain to failure compared to 386 MPa yield strength, 462 MPa ultimate strength, 8% elongation from literature [34]. As expected from the hardness tests, the as-welded sample exhibited a much lower yield strength of 246 MPa, ultimate strength of 349 MPa. A

total strain of 5% was observed in the as-welded material, with only work hardening and no necking, which is lower than would be expected from an annealed plate of Al 7075 T7351. Two of the as-welded samples fractured in the heat affected zone, while the third fractured in the weld ("As-Welded (i)" in Figure 4) – the sample that fractured in the weld provides an estimate for yield and ultimate strength for the TiC nanoparticle-enhanced Al 7075 material in the as-deposited condition of 235 MPa yield strength and 377 MPa ultimate strength. The other half of the welded plate, which was subjected to T73 heat treatment, was also prepared into tension tests. One sample fractured in the parent material, outside of the weld, with a yield strength of 412 MPa, close to the value of the parent material. This confirms the hardness results that the post heat-treated weld has mechanical properties that are indistinguishable from the parent alloy. This sample also provides information on the plastic strain experienced by the heat-treated weld material, with a 2.6% reduction in area and 1.3% lateral strain at the weld. The second of the heat-treated samples fractured in the weld ("Heat-treated (i)" in Figure 4), which could be thought of as an analog for the estimate of the 3D printed material if it had been fabricated into tension specimens. A 408 MPa yield strength, 448 MPa ultimate tensile strength and 5.8% total strain were observed for this sample. Table 3 summarizes the mechanical properties of the parent, as-welded, and heat-treated samples. A summary of the tensile properties obtained for this study are shown in Table 3.

4. Discussion and Conclusions

This work has proven the feasibility of using TiC nanoparticle-enhanced Al 7075 weld wire for fabricating crack-free welds of aluminum alloy 7075 with comparable properties to wrought material after T73 post-weld heat treatment, as confirmed by hardness and tension testing. Due to the small lattice mismatch between Al and TiC, the addition of the TiC nanoparticles serves to promote nucleation of the primary Al grains, resulting in a crack-free, fine equiaxed grain structure during solidification in the weld material after multi-pass welding, single-pass overlay, and multi-pass additive manufacturing – similar to what was shown for casting and welding by Zuo *et. al* [11] and Sokoluk *et. al* [17]. After solidification from the deposition processes, however, the weld material and parent plate have been exposed to thermal conditions that are not optimized for Al 7075 (i.e., slow cooling rate compared to a desired quench) and thus the mechanical properties of the as-deposited samples suffer due to uncontrolled precipitation of the secondary phase at the grain boundaries. Through the post-deposition T73 heat treatment, since the thermal conditions are optimized and controlled, the precipitates are redistributed uniformly throughout the grain structure and grain growth is inhibited by the TiC nanoparticles through grain boundary pinning – analogous to the results of the T6 heat treatment performed by Zuo *et. al* [11] and Sokoluk *et. al* [17] – resulting in returned hardness and strength of the weld and plate material after heat treatment to that of parent Al 7075 T73.

These results have major implications to the aerospace industry as it opens the path for conventional welding of highly-used Al 7075 T73. Furthermore, this work showcased the possibility of wire-based printing utilizing the TiC nanoparticle Al 7075 wire for use in overlays and wire-based AM. Thus, welding of Al 7075, either wrought-to-wrought, AM-to-wrought, or AM-to-AM has been shown as a possibility. Further research into welding of

multi-manufacturing process Al 7075 parts, with a goal of producing complex, high-strength aluminum parts (e.g., complex part to wrought spacecraft chassis) is of great interest, as this eliminates the need for bonding, brazing, bolting and fastening of Al 7075 components. Figure 5 shows future directions potentially enabled by this work: 1) wire-based additive manufacturing of Al 7075 and 2) conventional TIG welding of wrought and additively manufactured Al 7075 parts.

Future work involves mass production of the nano-reinforced Al 7075 feedstock wire and then manufacturing large Al 7075 parts using wire arc additive manufacturing (WAAM). Understanding the effect of machine parameters (e.g., layer height, deposition speed) will lead to finer control of part geometry and features. Additionally, the development and testing of other nanoparticle-enhanced alloys is of great interest. The development of the TiC nanoparticle-enhanced Al 7075 weld wire has showcased the feasibility of using nanoparticles to control the solidification of a previously unweldable alloy – it is of great interest to explore other precipitation hardened alloys, or other material classes, to see if solidification control via nanoparticles can result in novel processing methods such as welding or additive manufacturing.

In summary, this work explored the feasibility of fabricated welds, overlays, and 3D printed analog of Al 7075, with the following results:

1. Welding of common spacecraft aluminum 7075 T73 is possible utilizing TiC nanoparticle-enhanced Al 7075 weld wire and return of mechanical properties is possible through post-weld T73 heat treatment
2. Fabrication of Al 7075 T73 through a wire-based additive manufacturing process with properties similar to wrought material
3. Quantification of preliminary mechanical properties for TiC nanoparticle-enhanced Al 7075 parts in the as-welded and T73 post-weld heat-treat conditions

Acknowledgement

This work was supported by a NASA Space Technology Research Fellowship. MetaLi LLC produced and provided the nanoparticle-enhanced aluminum 7075 welding rods. The work was completed at the Jet Propulsion Laboratory, California Institute of Technology, under contract with NASA. Reference herein to any specific commercial product, process, or service by trade name, trademark, manufacturer, or otherwise, does not constitute or imply its endorsement by the United States Government or the Jet Propulsion Laboratory, California Institute of Technology.

References

1. Davis JR Aluminum and aluminum alloys in Alloying: understanding the basics 351–416 (ASM International, 2001).
2. Billing P. & Fleischner C. Mars science laboratory robotic arm. in Proceedings of 14th european space mechanisms and tribology symposium http://esmats.eu/esmatspapers/pastpapers/pdfs/2011/billing.pdf (2011).
3. Lindemann RA & Voorhees CJ Mars exploration rover mobility assembly design, test and performance. in Proceedings of IEEE international conference on systems, man and cybernetics 10.1109/ICSMC.2005.1571187 (2005).
4. Starke EA & Staley JT Application of modern aluminum alloys to aircraft. Prog. Aerosp. Sci. 32, 131–172 10.1016/0376-0421(95)00004-6 (1996).

5. Jawalkar CS & Kant S. A review on use of aluminum alloys in aircraft components. i-Manager's Journal on Material Science 3, 33–38 10.26634/jms.3.3.3673 (2015).
6. anigrahi SK & Jayaganthan R. Development of ultrafine grained high strength age hardenable Al 7075 alloy by cryorolling. Mater. Design 32, 3150–3160 10.1016/j.matdes.2011.02.051 (2011).
7. Ambriz RR & Jaramillo D. Mechanical behavior of precipitation hardened aluminum alloys welds in Light metal alloys applications (ed. Monteiro WA) 10.5772/58418 (IntechOpen, 2014).
8. Çevik B. Gas tungsten arc welding of 7075 aluminum alloy: microstructure properties, impact strength, and weld defects. Mater. Res. Express 5, 066540 10.1088/2053-1591/aacbbc (2018).
9. Ambriz RR & Mayagoitia V. Welding of aluminum alloys. in Recent trends in processing and degradation of aluminum alloys (ed. Ahman Z) 63–86 10.5772/18757 (2011).
10. Kang M. & Kim C. A review of joining processes for high strength 7xxx series aluminum alloys. J. Welding and Joining 35, 79–88 10.5781/JWJ.2017.35.6.12 (2017).
11. Zuo M. et al. Microstructure control and performance evolution of aluminum alloy 7075 by nano-treating. Sci. Rep. 9, 10671 10.1038/s41598-019-47182-9 (2019). [PubMed: 31337848]
12. Zhang MX, Kelly PM, Easton MA, & Taylor JA Crystallographic study of grain refinement in aluminum alloys using the edge-to-edge matching model. Acta Mater. 53, 1427–1438 10.1016/j.actamat.2004.11.037 (2005).
13. Rao AKP, Das K, Murty BS, & Chakraborty M. Al-Ti-C-Sr master alloy - a melt inoculant for simultaneous grain refinement and modification of hypoeutectic Al-Si alloys. J. Alloys Compd. 480, 147–149 10.1016/j.jallcom.2009.02.147 (2009).
14. De Cicco MP, Turng L-S, Li X, & Perepezko JH Nucleation catalysis in aluminum alloy A356 using nanoscale inoculants. Metall. Mater. Trans. A 42, 2323–2330 10.1007/s11661-011-0607-1 (2011).
15. Martin JH et al. 3D printing of high-strength aluminium alloys. Nature 549, 365–369 10.1038/nature23894 (2017). [PubMed: 28933439]
16. Choi H, Cho W, Konishi H, Kou S, & Li X. Nanoparticle-induced superior hot tearing resistance of A206 alloy. Metall. Mater. Trans. A 44, 1897–1907 10.1007/s11661-012-1531-8 (2013).
17. Sokoluk M, Cao C, Pan S, & Li X. Nanoparticle-enabled phase control for arc welding of unweldable aluminum alloy 7075. Nat. Commun. 10, 1–8 10.1038/s41467-018-07989-y (2019). [PubMed: 30602773]
18. Kaufman JG Understanding the aluminum temper designation system in Introduction to aluminum alloys and tempers 39–76 (ASM International, 2000).
19. Herderick E. Additive manufacturing of metals: a review. in Proceedings of materials science and technology conference and exhibition (2011).
20. Gibson I, Rosen D. & Stucker B. Additive manufacturing technologies: 3D printing, rapid prototyping, and direct digital manufacturing 2nd edn. 10.1007/978-1-4939-2113-3 (Springer, 2015).
21. Herzog D, Seyda V, Wycisk E, & Emmelmann C. Additive manufacturing of metals. Acta Mater. 117, 371–392 10.1016/j.actamat.2016.07.019 (2016).
22. Ding D, Pan Z, Cuiuri D, & Li H. Wire-feed additive manufacturing of metal components: technologies, developments and future interests. Int. J. Adv. Manuf. Technol. 81, 465–481 10.1007/s00170-015-7077-3 (2015).
23. Rodrigues TA, Duarte V, Miranda RM, Santos TG, & Oliveira JP Current status and perspectives on wire and arc additive manufacturing (WAAM). Materials 12, 1121 10.3390/ma12071121 (2019).
24. Geng H, Li J, Xiong J, Lin X, & Zhang F. Optimization of wire feed for GTAW based additive manufacturing. J. Mater. Process. Tech. 243, 40–47 10.1016/j.jmatprotec.2016.11.027 (2017).
25. Aboulkhair NT et al. 3D printing of aluminium alloys: additive manufacturing of aluminium alloys using selective laser melting. Prog. Mater. Sci. 106, 100578 10.1016/j.pmatsci.2019.100578 (2019).
26. Zhang D. et al. Metal alloys for fusion-based additive manufacturing. Adv. Eng. Mater. 20, 1–20 10.1002/adem.201700952 (2018).

27. Aversa A. et al. New aluminum alloys specifically designed for laser powder bed fusion: a review. Materials 12, 10.3390/ma12071007 (2019).
28. Wanhill RJH, Byrnes RT & Smith CL Stress corrosion cracking (SCC) in aerospace vehicles. in Stress corrosion cracking: theory and practice (ed. Raja VS & Shoji T.) 10.1533/9780857093769 (2011).
29. Dunn BD Materials and processes for spacecraft and high reliability applications (Springer, 2016)
30. Lin L, Liu Z, Han X, & Liu W. Effect of overaging on fatigue crack propagation and stress corrosion cracking behaviors of an Al-Zn-Mg-Cu alloy thick plate. J. Mater. Eng. Perform. 27, 3824–3830 10.1007/s11665-018-3518-0 (2018).
31. Park JK & Ardell AJ Microstructures of the commercial 7075 AI alloy in the T651 and T7 tempers. Metall. Trans. A 14, 1957–1965 10.1007/BF02662363 (1983).
32. Fu G, Tian F. & Wang H. Studies on softening of heat-affected zone of pulsed-current GMA welded Al-Zn-Mg alloy. J. Mater. Process. Technol. 180, 216–220 10.1016/j.jmatprotec.2006.06.008 (2006).
33. Avner SH Introduction to physical metallurgy (McGraw Hill, 1974).
34. Muraca RF & Whittick JS Materials data handbook: aluminum alloy 7075 https://ntrs.nasa.gov/archive/nasa/casi.ntrs.nasa.gov/19720022809.pdf (Western Applied Research and Development, Inc, 1972).

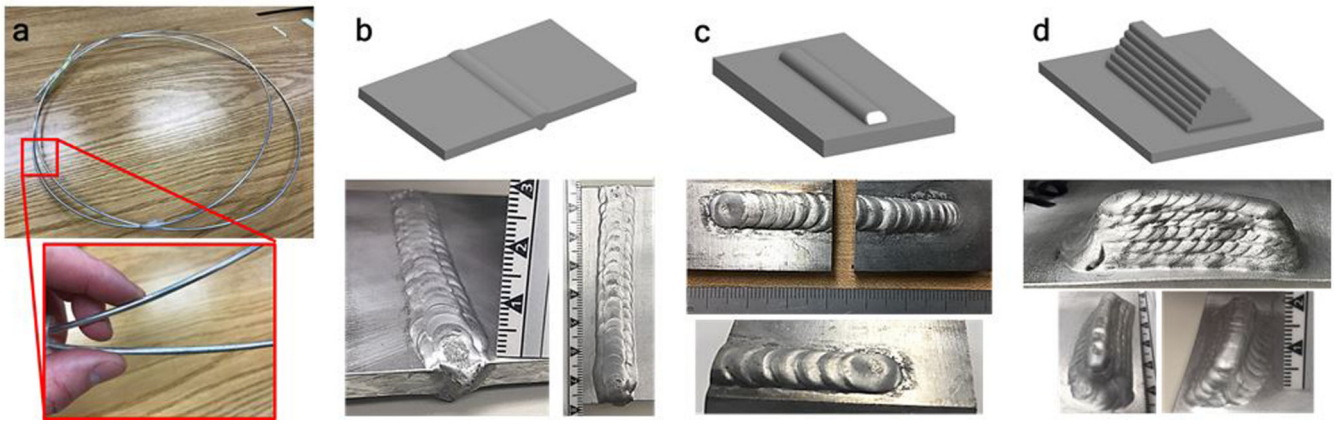

Figure 1 –.

Feedstock and fabricated samples: (a) TiC nanoparticle-enhanced weld wire, (b) conventional butt weld, (c) single layer overlay, (d) 3D printed multi-layer part

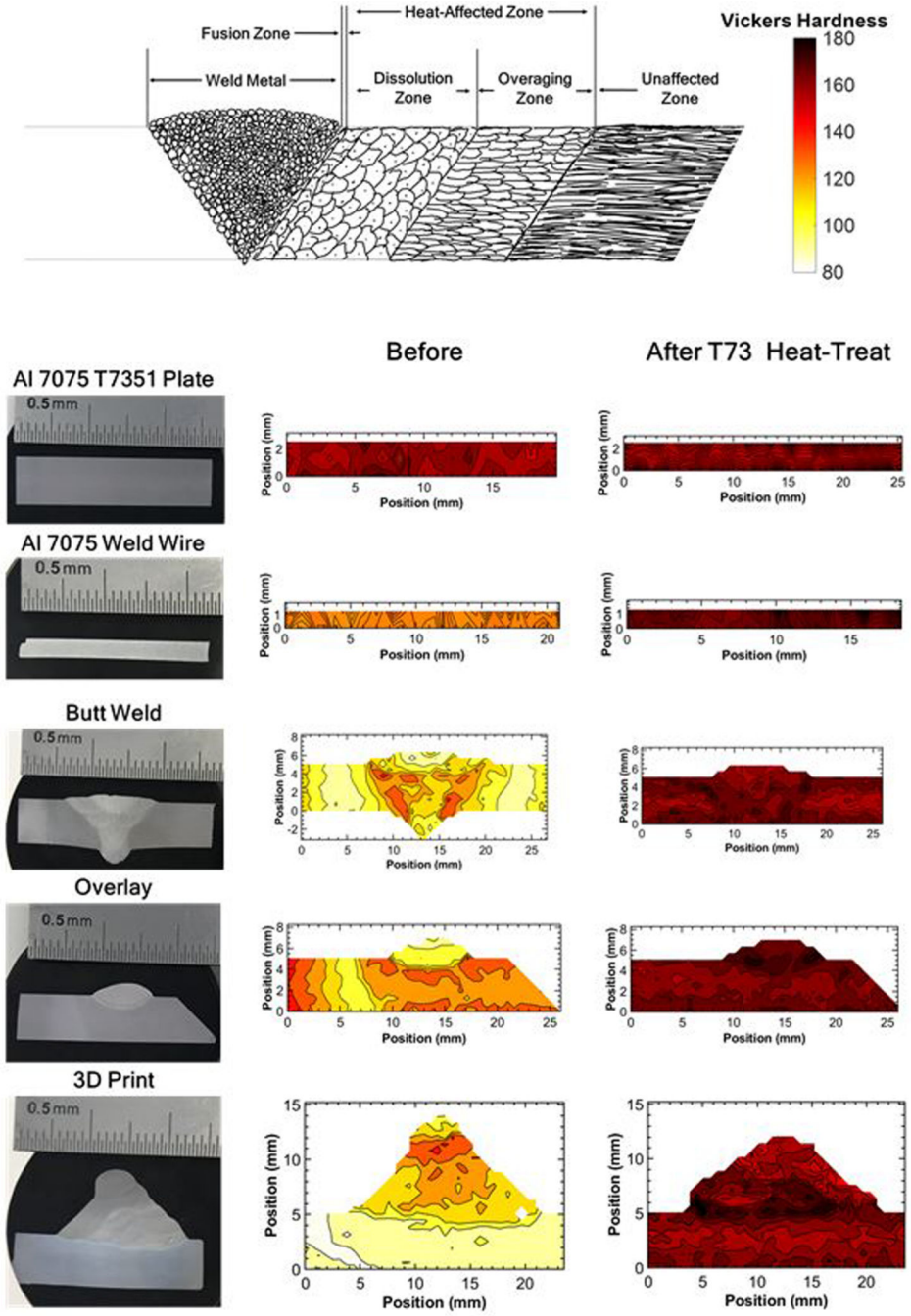

Figure 2 –.

Exemplary microstructure for weld using nanoparticle-enhanced wire (not to sale), optical images for feedstock and fabricated samples, and hardness mapping for feedstock and fabricated samples before and after T73 heat treatment

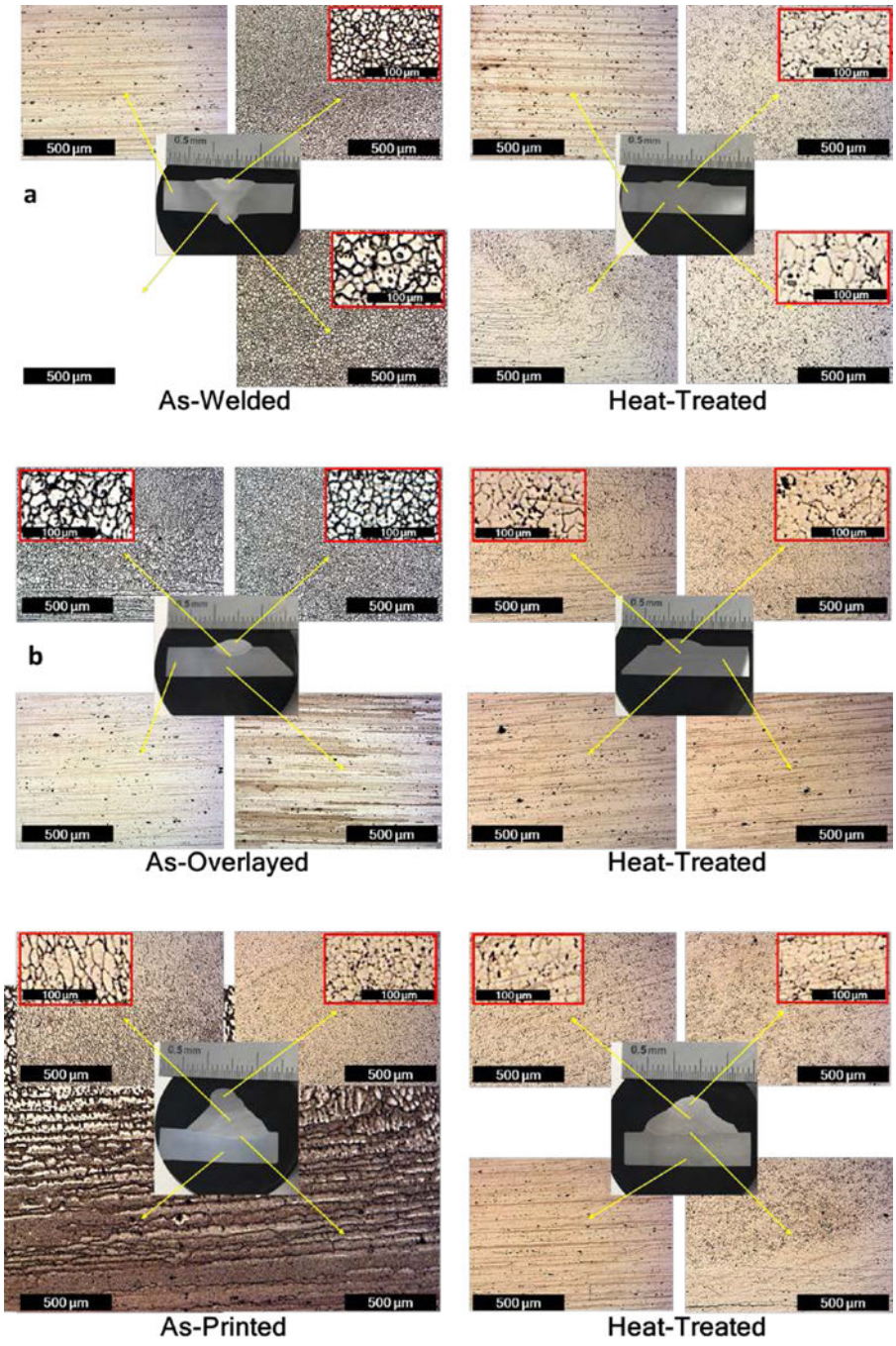

Figure 3 –.

Microstructure images for (a) conventional butt weld, (b) single layer overlay, and (c) 3D printed part before and after T73 heat treatment

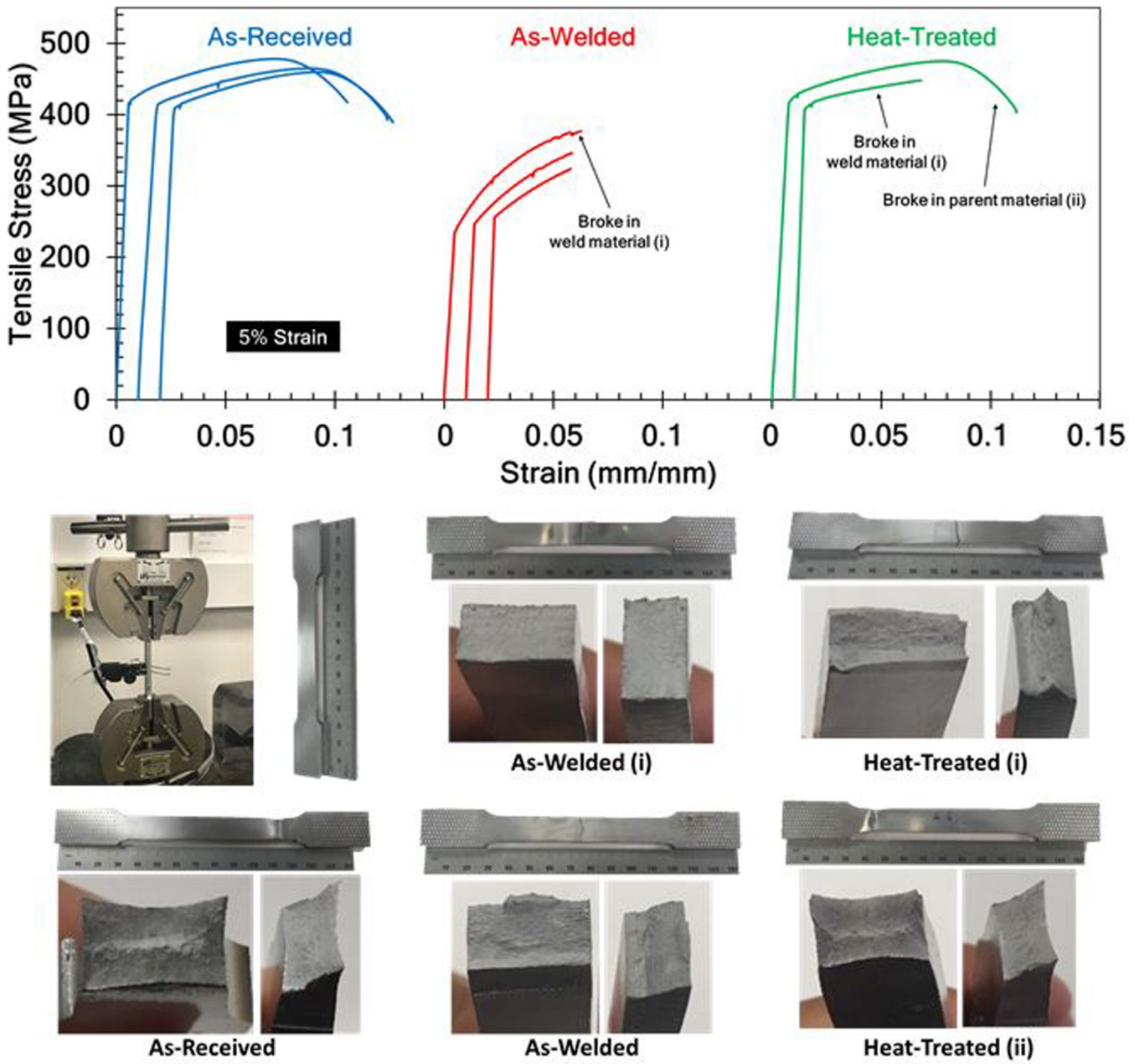

Figure 4 –.

Stress-strain data and fracture images for tensile samples of as-received plate, as-welded, and T73 heat-treated samples

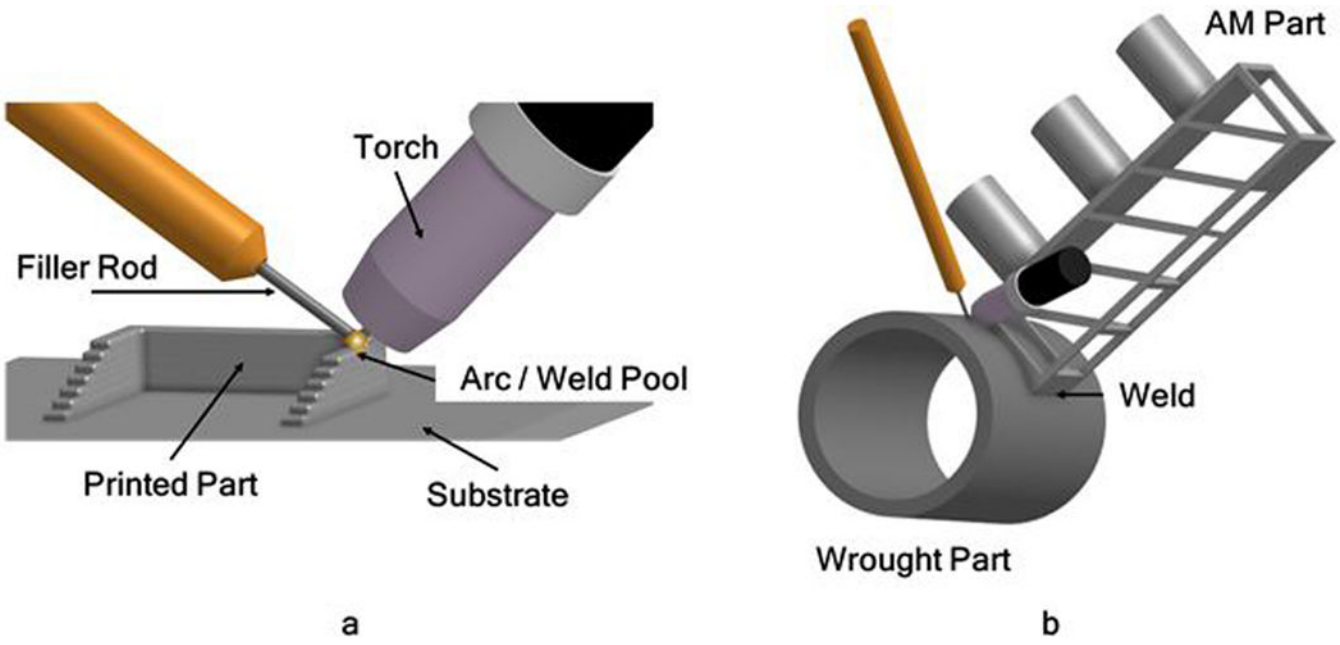

Figure 5 –.

Potential uses for nano-reinforced Al 7075 weld wire based on the current work include (a) wire arc additive manufacturing and (b) wrought-to-AM welding of Al 7075

Table 1 –

TIG Welding Parameters

Parameter	Values
Type of Current	Alternating Current
Max Current	180 Amps
Current Control	Pedal
Output Frequency	180 Hz
Balance	80%
Argon Flow Rate	30 cc/min
Electrode Gap	2.54–3.18 mm
Electrode Forward Speed	254 mm/min
Electrode	3/32” Tungsten Electrode
Ceramic Cup Size	#5

Table 2 –

Hardness values for conventional butt weld, single layer overlay, and 3D printed part before and after T73 heat treatment

Sample	Condition	Region	HV (Avg ± σ)
Parent Alloy	As-Received	Full Sample	160 ± 5
Butt Weld	As-Deposited	Weld Material	117 ± 12
	As-Deposited	Softest HAZ Region	95 ± 2
	Heat-Treated	Weld Material	165 ± 5
Single Layer Overlay	As-Deposited	Weld Material	104 ± 5
	As-Deposited	Softest HAZ Region	105 ± 3
	Heat-Treated	Weld Material	168 ± 5
3D Print	As-Deposited	Weld Material	120 ± 9
	As-Deposited	Softest HAZ Region	86 ± 2
	Heat-Treated	Weld Material	163 ± 9

Table 3 –

Tensile properties for as-received Al 7075 T7351 plate, as-welded Al 7075, and T73 heat-treated Al 7075 samples

	Yield Strength (MPa)	Ultimate Tensile Strength (MPa)	Total Strain (%)
Parent Al 7075 T73	413 ± 4	468 ± 10	11 ± 1
As-Welded	246 ± 11	349 ± 27	5 ± 1
Heat-treated	411 ± 6	462 ± 19	9 ± 4